JOURNAL OF THERMOPLASTIC COMPOSITE MATERIALS

Original Research Article

Journal of Thermoplastic Composite Materials
2026, Vol. 0(0) 1–33

DOI: 10.1177/08927057261415883
journals.sagepub.com/home/jtc
Sage

Advancing mechanical properties of thermoplastic biocomposites through tannic and gallic acids surface treatment of natural fiber reinforcements: A simulation and experimental study

Sultan Ullah[1], Giedrius Janusas[1], Christopher M Pastore[2], Raul Fangueiro[3], Arvydas Palevicius[1], Almontas Vilutis[4], Sandra Varnaitė-Žuravliova[5] and Justas Eimontas[6]

Abstract

This research explores the mechanical enhancement of thermoplastic biocomposites by altering the surface of natural fiber reinforcements using biodegradable acids, with a particular focus on flax and jute fibers treated with 2% potassium hydroxide (KOH) and various percentages (0%, 1.2%, 1.8% and 2.4%) of bio-based acids (tannic acid and gallic acid). These processed fibers were incorporated into a methyl methacrylate (MMA)-based thermoplastic matrix using hand layup followed by the compression

[1]Department of Mechanical Engineering, Faculty of Mechanical Engineering and Design, Kaunas University of Technology, Kaunas, Lithuania
[2]Kanbar College of Design, Engineering and Commerce, Thomas Jefferson University, Philadelphia, PA, USA
[3]Fibrenamics, Institute of Innovation on Fibre-Based Materials and Composites, University of Minho, Guimarães, Portugal
[4]Department of Engineering, UAB Poliplastas, Kaunas, Lithuania
[5]Department of Textile Technologies, Center for Physical Sciences and Technology, Kaunas, Lithuania
[6]Combustion Process Laboratory, Lithuanian Energy Institute (LEI), Kaunas, Lithuania

Corresponding authors:
Sultan Ullah, Department of Mechanical Engineering, Faculty of Mechanical Engineering and Design, Kaunas University of Technology, Kaunas, Lithuania.
Email: sultan.ullah@ktu.edu

Giedrius Janusas, Department of Mechanical Engineering, Faculty of Mechanical Engineering and Design, Kaunas University of Technology, Kaunas, Lithuania.
Email: giedrius.janusas@ktu.lt

molding to fabricate a composite to achieve 1.97 mm thickness. Surface characterisation using FTIR and TGA demonstrated successful modification of fiber surfaces, improving fiber-matrix bonding. A series of mechanical tests evaluating tensile, flexural, impact, and abrasion behavior demonstrated significant property improvements in the composites. The most consistent and favorable outcomes were achieved with a 1.8% acid treatment, which enhanced critical metrics including tensile strength (60.57 MPa), flexural modulus (5.91 GPa), and impact resistance (8.34 kJ/m^2). Finite element analysis (FEA) provided a corroboration for these experimental findings with simulations and the errors obtained when comparing results of maximum stress are approximately 1-3%. Collectively, this evidence positions biodegradable acid treatments as a viable and sustainable method for advancing the performance of natural fiber-reinforced composites toward practical use.

Keywords
Thermoplastic biocomposites, surface modification, mechanical properties, finite element analysis, abrasion resistance, sustainable materials

Introduction

The rising global concern over non-degradable synthetic materials has positioned renewable fibers as promising alternatives in composite applications, primarily because of their biodegradability and lower ecological impact.[1,2] Among them, flax and jute are bast fibers extracted from the stems of Linum usitatissimum and Corchorus plants, respectively. These natural fibers serve as a sustainable substitute for synthetic reinforcements, requiring less energy to produce and resulting in fewer greenhouse gas emissions.[3,4] They also present distinct practical and economic advantages, characterized by their low cost, minimal weight, natural biodegradability, and wide availability. A primary obstacle to their wider adoption, however, is their natural affinity for water. This hydrophilic tendency results in absorbed moisture that causes the fibers to swell, weakens their bond with the matrix, and induces dimensional instability in the final composite, all of which deteriorate its mechanical properties.[5] Although these issues currently limit natural fibers' capacity to displace synthetics,[6–12] targeted surface modifications present a viable solution.[13] Such treatments strengthen the fiber-matrix bond, significantly improving the composite's mechanical strength and wear resistance.[14,15] When implementing surface modification techniques, careful consideration of chemical compatibility, treatment duration, processing conditions, and material handling is essential.[16–18] Surface modifications of natural fibers have two fundamental approaches: physical and chemical.[19] Physical methods alter only the surface morphology and properties without changing the chemical composition such as plasma, UV/irradiation, heat treatment, and surface fibrillation.[20–22] Chemical treatment techniques which change the crystallinity, surface chemistry and introduce new functional groups include mercerization (alkali treatment), silane, benzoylation, and acetylation etc..[23] For instance, alkali treatment improves

natural fibers by roughening the surface and removing impurities.[24] However, traditional sodium hydroxide (NaOH), especially at elevated temperatures, often damages the fiber structure and weakens its mechanical properties. In contrast, potassium hydroxide (KOH) has emerged as a promising, milder alternative. By carefully controlling processing parameters, KOH treatment removes impurities without significantly compromising the cellulose integrity, resulting in less fiber degradation and enhanced mechanical performance.[25] Therefore, chemical treatments indicate a highly recommended strategy for addressing the deficiencies of biocomposites.[26]

Gallic acid (GA), a single-molecule phenolic acid,[27] and tannic acid, its complex polyphenolic derivative, have both emerged as promising bio-based agents for improving the mechanical performance of biocomposites, serving as sustainable partial replacements for petroleum-based phenol.[28] As an eco-friendly alternative, natural and abundant gallic acid molecule has the ability to enhance a slight increase in mechanical integrity of biocomposites specifically stiffness' and tensile strength, backing immobilization of iron phenlyphosponate on flax fiber along with thermal properties.[29] Raja et al. found that incorporating higher amount of GA in poly (butylene adipate-co-terephthalate) (PBAT) composite film enhanced the mechanical strength, oxygen barrier properties, hydrophobicity and antibacterial activity.[30] Derivates of GA in polymeric composite films improve their stability by limiting their swelling and degradation, which is attributed to increase the physical interactions and hydrogen bonding.[31] In the work of M. Zhang et al., which resulted in 78.7% enhancement in interfacial shear strength in carbon fiber reinforced polymer composites with bio-based GA derivates.[32] A. M Croitoru et al., researched on the fabrication of fibers with various concentrations of GA for evaluating antimicrobial, mechanical and their compatibility with other materials.[33] In a study by Liu et al., it demonstrated a marked improvement in the mechanical properties of carbon fiber/epoxy composites with GA derivates increasing interlaminar shear strength by 14%, flexural modulus by 13%, and flexural strength by 27%.[34] Research by B. Pishva et al. demonstrated the immobilization of GA derivatives on polycaprolactone (PCL), resulting in a scaffold that integrates the structural integrity of PCL nanofibers with the bioactivity of GA.[35] S. Chen et al. developed gallic-acid based epoxy resin (GA-ER) and found better tensile and impact properties of composites than their pure counterparts, positioning it a viable alternative to common epoxies.[36]

By altering the chemistry of natural fibers, the polyphenolic molecule tannic acid (TA) acts as an effective agent for improving strength, adhesion, and composites durability.[37] Kamaludin et al., worked on the fabrication of TA treated biocomposites using compression molding, resulted in improved tensile, thermal, water absorption, and structural properties.[38] In the study on biocomposites, Shibata et al., reported a significant improvement in tensile strength, and tensile modulus following treatment with TA under different conditions.[39] Scientific results obtained by Kim et al., employing a TA-based epoxy in carbon fiber reinforced plastic (CFRP) fabrication improved the interfacial bonding between the constituents, resulting in better mechanical properties.[40] Hu et al., worked on the enhancement of interfacial adhesion of carbon fiber reinforced composites using ferric ion and TA treatment, achieving 80% improvement in interfacial shear strength.[41] Xiang et al., researched on modified basalt fiber-reinforced polymer (BFRP)

composites through TA and aminopropyltriethoxysilane (APS), obtained interfacial shear strength (IFSS) increases by 65.3%, contributing to improvement of 38.1% in flexural strength, 31.6% in flexural modulus, and 20.9% interlaminar shear strength, respectively.[42] According to Singh et al., integration of tannic acid treated bamboo micron fibers (TBMFs) as a hybrid component in glass fiber reinforced plastics (GFRP) resulted in a substantial enhancement of mechanical properties, with yield strength (σ_y) and elastic modulus (E) increasing by 48% and 55%, respectively, over the untreated composite.[43] Liu et al. strengthened and toughened the bamboo fibers reinforced poly (lactic acid) (BF/PLA) biocomposites evaluating mechanical performances such as tensile strength, impact strength, thermomechanical properties utilized a TA-crosslinked epoxidized soybean oil (TA-ESO).[44] This study investigates a novel chemical approach for enhancing biocomposites, focusing on the unexplored effects of KOH treatment combined with tannic acid-treated jute and gallic acid-treated flax in an MMA-based thermoplastic matrix. The research comprehensively evaluates mechanical properties (tensile, flexural, impact, abrasion), thermal behavior and microstructure, supported by computational modeling of experimental data. Future work will focus on scaling up the fabrication process and evaluating the long-term durability of these composites under real-world environmental conditions.

Materials and methods

Raw materials

Natural reinforcements such as plain-woven jute and flax were obtained from the Department of Mechanical Engineering, KTU, Kaunas, Lithuania, while liquid reactive MMA thermoplastic resin (Elium151 XO/SA), supplied by Arkema, Colombes, France. Some of the physical and mechanical properties of natural fibers flax and jute are summarised in Table 1, Table 2, respectively.

The apparent modulus measures the fabric's stiffness in its woven form. The Elium151 XO/SA resin system comprises three components: 151 XO resin, 151 SA accelerator, and a peroxide initiator. Upon the integration of all three parts, radical polymerisation starts, resulting in a poly (methylmethacrylate) (PMMA) thermoplastic

Table 1. Physical and mechanical properties of woven flax fabrics.

Properties/Features	Value
Fiber density	1.45 ± 0.02 g/cm^3
Areal density	212.5 g/m^2
Elongation at break	1.3%
Water content[a]	5–7%
Apparent modulus	58 ± 2 GPa

[a]Valid under the following conditions: 22°C, 50% RH.

matrix. The initiator employed in this research was Butanox M-50, a medium-reactive, general-purpose methyl ethyl ketone peroxide (MEKP) solution in dimethyl phthalate, procured from Ecocompósitos, SA, Faro, Portugal. The typical cured non-reinforced Elium resin properties are detailed in Table 3.

Potassium hydroxide (KOH), acetone and distilled water were used for the cleaning and washing of fabrics. To enhance the fiber-matrix bonding interaction tannic acid (TA) and gallic acid (GA) was obtained from Sigma-Aldrich (reagent grades: CAS# 1401-55-4, Mol. Wt.1701.20 for TA and CAS# 149-91-7, Mol. Wt.170.12 for GA), St Louis, MO, USA.

Surface treatment and sampling sequence of natural fiber reinforcements

Reinforcement layers of both flax and jute, measuring 6“ × 6”, were cut and washed with distilled water to eliminate intrinsic impurities. The layers were distinctively etched in a 2% KOH solution [25] at 40°C for 80 minutes and then rinsed with distilled water before oven drying. After drying, the jute specimens were subjected to tannic acid (TA) treatment based on their weight, utilising various concentrations and durations, while the flax specimens underwent gallic acid (GA) treatment under similar conditions, as detailed in Table 4, employing mild sonication. The treatment was conducted at room temperature, maintaining a pH of 8 throughout the process.

Table 2. Physical and mechanical properties of woven jute fabrics.

Properties/Features	Value
Fiber density	1.45 ± 0.03 g/cm^3
Areal density	259.5 g/m^2
Elongation at break	1.5–2.0%
Water content[a]	8–10%
Apparent modulus	30 ± 2 GPa

[a]Valid under the following conditions: 22°C, 50% RH.

Table 3. Properties of typically cured non-reinforced Elium151 XO/SA polymer.

Properties/Features	Value
Heat deflection temperature	75.90°C
Tensile strength	47.00 MPa
Tensile modulus	2.6–2.70 GPa
Tensile elongation at break	4.3–4.6%
Flexural strength	80.00–81.50 MPa
Flexural modulus	2.6–2.7 GPa
Flexural elongation	4.42%

Fabrication of hybrid biocomposites

The tannic acid treated jute and the gallic acid treated flax fabrics were incorporated in the fabrication of four-ply laminated hybrid biocomposite materials through hand layup and compression molding methods for mechanical testing including tensile, flexural and Charpy pendulum impact tests as shown in Table 5. Thermoplastic polymer was applied, and four plies (Jute/flax/Jute/flax) were assembled in a 6″ × 6″ configuration for each specimen using hand layup. Subsequent to hand layup, these plies were positioned in the hot plates of a compression molding machine to cure the bio-composites at 60°C under an initial pressure of 2 kN for 10 minutes, followed by an increase to 12 kN for 40 minutes. The hot press was permitted to cool to ambient temperature while under applied pressure. For abrasion test of composites, 2 layers biocomposites were prepared, and method of fabrication was the same using hand layup and compression molding. Figure 1 shows the comprehensive approach and photographs captured throughout the process.

Table 4. Treatment performed with tannic and gallic acids for jute and flax fabrics at different concentrations and processing times.

Sr No.	Fabric type	Treatment group	Acid type	Acid concentration	Processing time
1	Jute	Untreated	N/A	N/A	N/A
2	Jute	Treated	Tannic acid	1.2%	10 min
3	Jute	Treated	Tannic acid	1.8%	15 min
4	Jute	Treated	Tannic acid	2.4%	20 min
5	Flax	Untreated	N/A	N/A	N/A
6	Flax	Treated	Gallic acid	1.2%	15 min
7	Flax	Treated	Gallic acid	1.8%	20 min
8	Flax	Treated	Gallic acid	2.4%	70 min

Table 5. Details of fabricated hybrid biocomposites for mechanical testing including tensile, flexural and Charpy pendulum impact tests.

Sample code	Reinforcement	Alkaline treatment	Jute ply acid treatment	Flax ply acid treatment
JFTG0	2 layers of jute, 2 layers of flax (J/F/J/F [0/90/0/90])	2% KOH	Nil	Nil
JFTG1.2	2 layers of jute, 2 layers of flax (J/F/J/F [0/90/0/90])	2% KOH	1.2% TA	1.2% GA
JFTG1.8	2 layers of jute, 2 layers of flax (J/F/J/F [0/90/0/90])	2% KOH	1.8% TA	1.8% GA
JFTG2.4	2 layers of jute, 2 layers of flax (J/F/J/F [0/90/0/90])	2% KOH	2.4% TA	2.4% GA

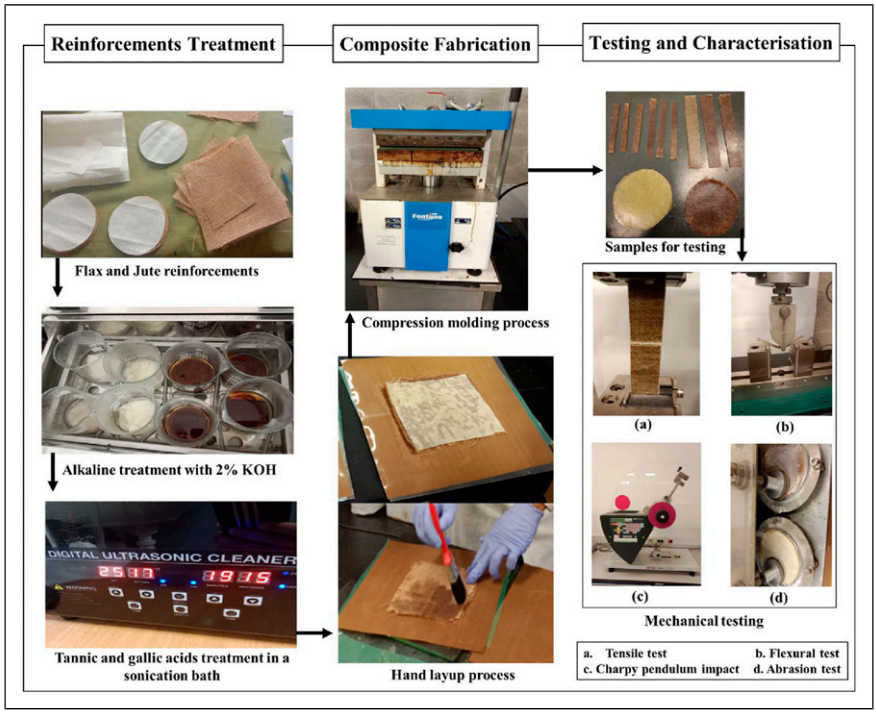

Figure 1. Scheme of biocomposites showing various steps during reinforcements treatment, fabrication process, and testing.

Characterisation of fabrics/reinforcements

The fabric characterisation of both reinforcements was conditioned in a standard atmosphere (20 ± 2°C temperature and 65 ± 4% relative humidity) according to LST EN ISO 139:2006 for 24 hours prior to testing. Fabrics tensile strength was measured following the strip test method in accordance with LST EN ISO 13934-1:2013, and the fabric weight in grams per square meter (GSM) was determined following LST EN 12127:1999. Tensile tests were conducted on the SDL Atlas M350-10AX universal testing machine (SDL Atlas Ltd, USA). Abrasion tests were assessed on the James H Heal N-Martindale 404 abrasion tester for fabrics under standard LST EN 1SO 12947-2:2017. Sample cutting for shrinkage was performed using the standard LST EN ISO 3759:2011. Fabric shrinkage, post-washing was assessed according to ISO 5077:2008 WASCATOR FOM71MP, FTMC, Kaunas, Lithuania. Washing (40 ± 3°C) at normal agitation and line drying (vertical) operation carried out employing the standard method LST EN 6330: 2022. Performing the standard process, Fourier Transform Infrared (FTIR) spectroscopy was executed out by an IR Tracer 100 spectroscope (Shimadzu, Columbia, MD, USA) to assess the impact of chemicals on fabrics. Thermogravimetric analysis (TGA) was performed on a STA 449 F3 Jupiter at Lithuanian Energy Institute (LEI), Kaunas. The weight loss of the control and fabrics was

recorded from room temperature to 900°C at a heating rate of 10°C/min under nitrogen atmospheres. These standardised methodologies presented the uniform and precise description of the materials for subsequent studies.

Evaluation, testing and modeling of composites

The mechanical behaviour of the composites was evaluated through tensile, flexural, and impact testing in Fibrenamics Association – Institute for Innovation in Fibrous and Composite Materials, Portugal. Tensile tests were evaluated using a universal testing machine at an extension rate of 2 mm/min accordance with ASTM D3039, employing specimens of 152.4 mm × 25 mm. Flexural properties were determined using a three-point bending setup at a crosshead speed of 1 mm/min following ASTM D7264, with specimen dimensions of 120 mm × 13 mm. Charpy impact testing was performed on samples measuring 100 mm × 10 mm at an impact velocity of 3.7 m/sec according to ISO 179-1. Thermogravimetric analysis (TGA) was carried out in a nitrogen atmosphere at a constant heating rate to assess thermal stability and weight loss behaviour. Fracture morphology and damage mechanisms were examined using an FEI Nova 200 NanoSEM (FEG/SEM) at the SEMAT facility, University of Minho, Portugal. Numerical simulation using ANSYS software were employed to validate the experimental tensile and flexural responses of the composites.

Results and discussion

Characterisation of biocomposite reinforcements

FTIR spectroscopy for fabrics. The FTIR analysis of jute fabric processed with various concentrations of tannic acid (TA) and flax fabric treated with gallic acid (GA) as indicated in Figure 2 provide details on the chemical alterations induced by these processing. Key functional groups, such as the OH stretching (3334 cm^{-1}), C = C stretching (2334 cm^{-1}), C = O stretching (1598 cm^{-1}) demonstrated the tannic and gallic acids adherence to the fiber surfaces (approximately 1500 and 2000 cm^{-1}), and C-O-C stretching (1164 cm^{-1}), identify the interactions between the respective bio-acids and the constituents of natural fibers. Various bonds such as ester and ether are formed, and a change in the intensity of peaks observed after the application of tannic acids with jute fabric and gallic acids with flax fabric. These results propose that both tannic and gallic acids successfully crosslink with cellulose, enhancing the fibers structural integrity by creating new chemical bridges.

Natural fibers contain a chain of cellulose, and such treatments of acids with the fibers strengthen and stabilise it making a new chemical bridge. Because of this crosslinking process, natural fibers gains enhanced mechanical properties including higher tensile strength and resistance to deformation. The comparative analysis of both natural fibers highlights the significant influence of acids on structural property changes, emphasizing their role in enhancing the fibers' functional characteristics. In general, the FTIR spectrum shows that alkaline treatment with KOH successfully cleans the fiber surfaces by eliminating impurities like lignin, hemicellulose, and waxes, while maintaining the integrity of cellulose. These modifications improve the surface properties of flax and jute fabrics, making them more compatible with polymer matrices in composite applications.

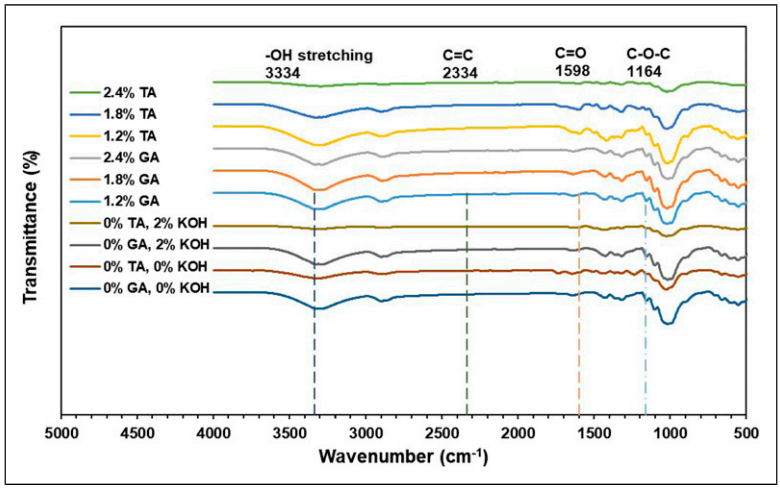

Figure 2. FTIR spectra of jute woven and flax fabrics treated with various concentrations of tannic acid and gallic acid.

Thermal analysis of reinforcements

Thermo gravimetric analysis (TGA) and derivative thermo gravimetric analysis (DTGA) were carried out to examine the degradation of natural fibers like jute and flax when treated with different concentrations of acids, with results shown in Figure 3. The thermal data obtained for fibers presents a potential enhancement in the stability of materials after acids treatment. The results demonstrate clearly the mass loss for the treated natural fibers thermal resistance and it's been improved. For flax fibers, increasing the concentration of GA improved thermal performance, resulting in less mass loss at higher temperatures. Thermal stability has a dependence on the higher concentrations of TA acids treatment with jute such as those processed with 1.8% and 2.4% exhibit greater thermal stability. Treatment of natural fibers with tannic acids and gallic acids facilitates the formation of bonds with the polymer and make the surface active and is attributed to the functionalisation of fibers. In parallel, these bonds are more resistant to breaking, leading to a higher degradation temperature. These findings highlight that both TA and GA treatments may improve the thermal stability of natural fibers, making them more viable for use in high-temperature composite material applications.[45,46]

Physical, tensile and abrasion properties of composite preform

Table 6 lists the physical properties of flax and jute fabrics in both warp and weft, comparing values before (F-BT, J-BT) and after (F-AT, J-AT) treatment with 2% KOH, respectively. Treatment with 2% KOH compacted both fabrics evidenced by shrinkage in flax (7.92% warp, 11.4% weft) and jute (5.09% warp, 3.5% weft) consistent with the

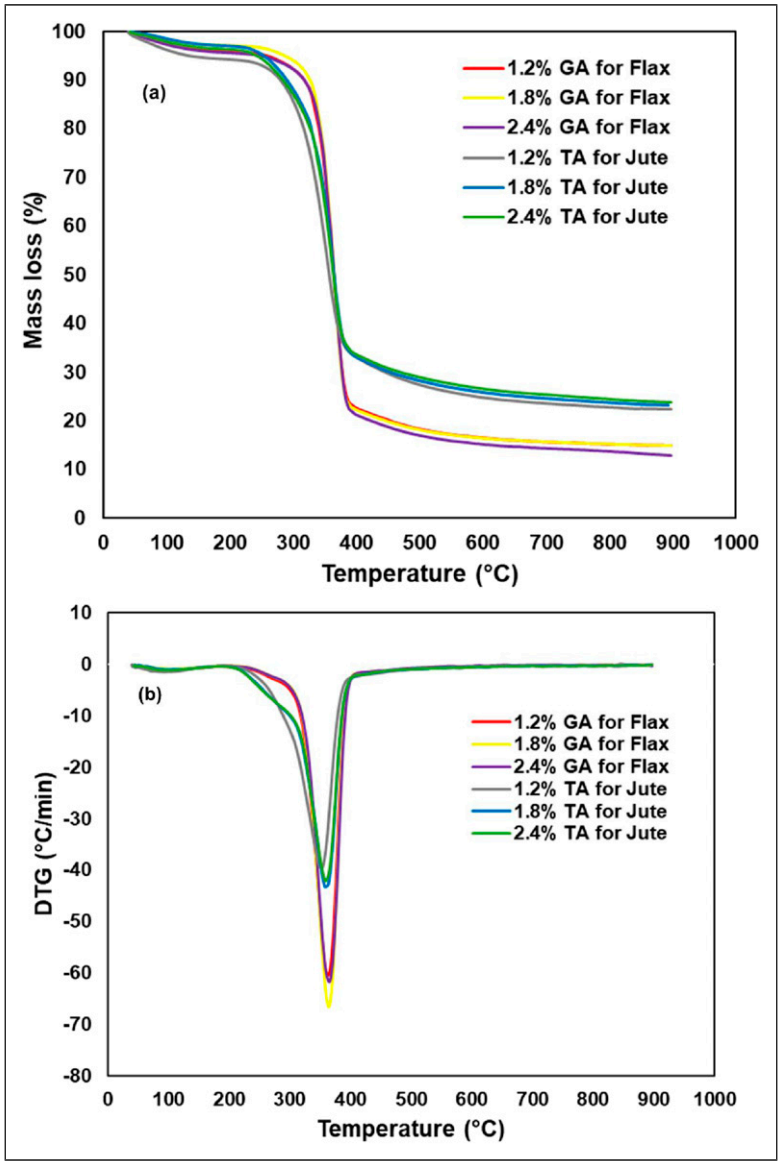

Figure 3. TG (a) and DTG (b) curves for jute and flax fabrics with different concentrations of acids treatment.

removal of surface waxes, hemicellulose, and portions of lignin that promotes closer yarn packing and higher inter fiber friction. This structural tightening was accompanied by reduced ply strength: flax declined from 826 to 817 N (warp) and 964 to 845 N (weft), and jute from 629 to 551 N (warp) and 682 to 621 N (weft), changes attributable to the loss of

Table 6. Physical properties of biocomposite preforms/fibers.

Sample code	Areal density (g/m^2)	Tensile strength (warp) (N)	Tensile strength (weft) (N)	Elongation (warp) (%)	Elongation (weft) (%)	Abrasion resistance (cycles)	Shrinkage (warp) (%)	Shrinkage (weft) (%)
F-BT	212.5	826	964	15.8	5.3	18000	___	___
F-AT	220	817	845	20.6	14.8	9000	7.92	11.4
J-BT	259.5	629	682	7.1	4.2	9500	___	___
J-AT	345	551	621	10.3	6.7	8000	5.09	3.5

non-cellulosic "cementing" constituents and partial cellulose I to II conversion that increases amorphous regions and microdefects. When normalised by areal density, the concept is clear: untreated flax carried more load per unit mass than jute (≈3.9–4.5 vs 2.4–2.6 $N.m^2.g^{-1}$), and all treated states were lower than their untreated analogues. Elongation at break increased after treatment (flax: 15.8 to 20.6% warp; 5.3 to 14.8% weft; jute: 7.1 to 10.3% warp; 4.2 to 6.7% weft), consistent with decreased yarn crimp and softer bundles; this may aid drape during lay-up but implies a lower initial modulus. Abrasion resistance (9 kPa) also deteriorated, more strongly in flax (18,000 to 9000 cycles) than in jute (9500 to 8000 cycles), indicating greater fibrillation and handling sensitivity.

Collectively, the data show that 2% KOH enhances surface readiness and fabric compactness for subsequent composite fabrication but compromises a slight change in intrinsic tensile and wear performance, with the trade-off being more pronounced for flax; for tensile-critical laminates, milder alkali better preserve cellulose integrity while maintaining adhesion. Furthermore, the normalised tensile strength ($N.m^2.g^{-1}$) as shown in Figure 4 is determined using the formula provided in equation (1):

$$Normalised\ tensile\ strength = \frac{Tensile\ strength}{Areal\ density} \tag{1}$$

Characterisation of biocomposites

Tensile properties. The tensile properties of untreated and phenolic acid-treated jute/flax hybrid biocomposites with different concentrations have been compared in Figure 5. The

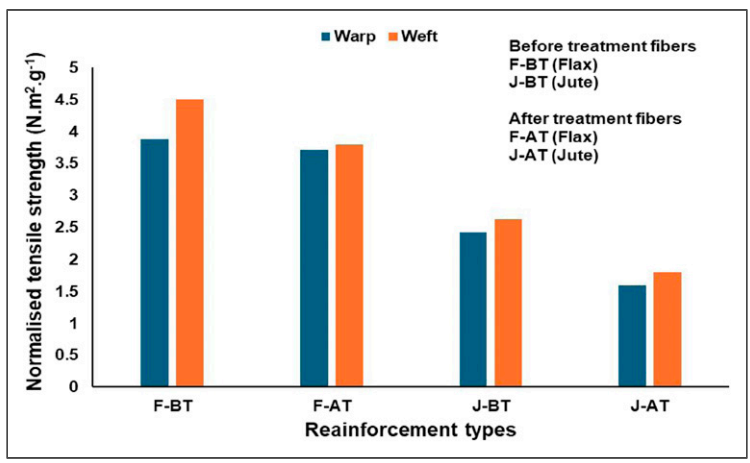

Figure 4. Normalised tensile strength of untreated (F-BT, J-BT) and treated (F-AT, J-AT) flax and jute reinforcements.

untreated sample (JFTG0) exhibited a tensile strength of 49.87 MPa and a modulus of 2.99 GPa, reflecting limited interfacial bonding between the untreated natural fibers and the Elium thermoplastic matrix. When the fibers were treated with tannic acid (TA) and gallic acid (GA), both properties improved noticeably, confirming the effectiveness of the surface modification. The enhancement can be attributed to improved fiber-matrix adhesion resulting from hydrogen bonding and possible esterification between the phenolic groups of TA/GA and the hydroxyl groups present on the cellulose surfaces of the fibers. Stress transfer ability between the polymer and the natural fibers has been enhanced due to the chemical interaction.

A biocomposite with 1.8% (JFTG1.8) concentration achieving a tensile strength of 60.57 MPa and a modulus of 4.20 GPa. This determines the moderate concentration and duration of TA and GA (1.8%) provides an optimal balance between surface activation and fiber integrity, improving wettability and load distribution with no degradation. Tannic and gallic acids alter the natural fibers structure by interacting with cellulose hydroxyl groups. This process has a dual effect. On one hand, it builds crosslinks that act as reinforcements within the cellulose network, significantly boosting the fiber's mechanical strength. On the other hand, it causes the fibers to clump together. If this clustering becomes excessive, the fibers lose their flexibility and become brittle, ultimately degrading their overall strength. While the treatment concentration reaches 2.4%, the material's strength and stiffness begin to deteriorate. At high level, the treatment itself starts to damage the fibers. This could either cause tiny structural flaws or make the fibers so rigid that the resin can't seep in properly, ultimately compromising the bond between them. As shown in Figure 6, the fractured surfaces of the tensile-tested specimens reveal that all samples experienced cross-grain fracture patterns.

In summary, the results clearly show that controlled bio-based acid treatment enhances the tensile performance of natural fiber-reinforced Elium composites. A treatment level

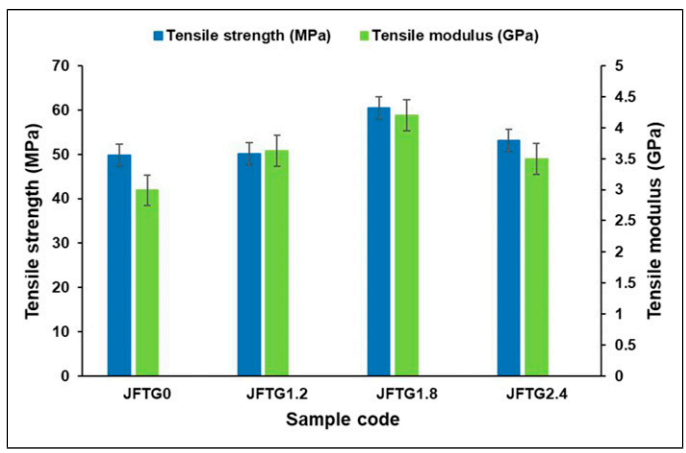

Figure 5. Influence of tannic and gallic acid concentration on the tensile properties of jute and flax biocomposites.

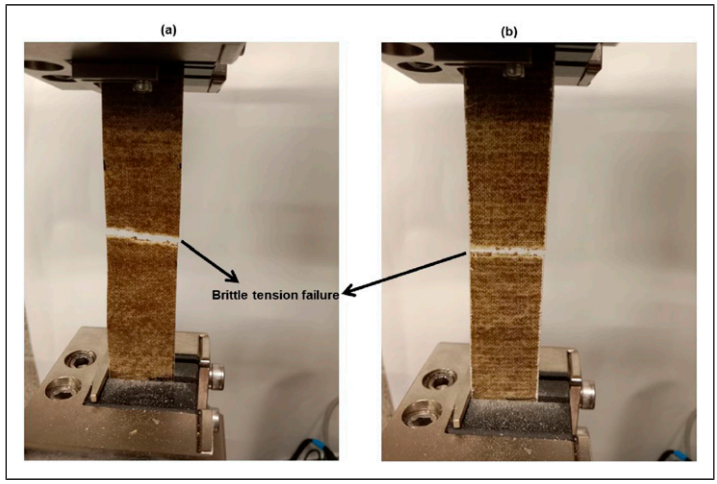

Figure 6. Tensile fractured specimens (a) JFTG0, and (b) JFTG1.8.

around 1.8 wt% of TA and GA maximises fiber-matrix adhesion and mechanical efficiency while maintaining the structural integrity of the reinforcement.

Figure 6 highlights the fractured surfaces of tensile characterised specimens for JFTG0 and JFTG1.8. A similar behavior observed for JFTG1.2 and JFTG2.4.

Flexural properties. Flexural properties of biocomposites are shown in Figure 7, indicating an improvement following the TA and GA treatment, compared to the untreated sample. These enhancements clearly reflect the influence of treatment concentration on fiber-matrix interfacial bonding. The untreated sample (JFTG0) exhibited a flexural strength of 61.66 MPa and a modulus of 3.31 GPa. The 1.2% acid treatment (JFTG1.2) resulted in a flexural strength of 74.66 MPa and a modulus of 4.47 GPa, demonstrating a significant enhancement in performance. These figures correspond to a roughly 21% gain in flexural strength and a 35% gain in modulus. The optimal concentration was 1.8% (JFTG1.8), which achieved the highest recorded values of 89.96 MPa for strength and 5.91 GPa for modulus. This marks a substantial gain of about 46% in strength and 79% in modulus compared to the untreated material. However, a slight downturn in properties at the 2.4% concentration (JFTG2.4) points to the beginnings of over-treatment.

The consistent improvement up to the 1.8% mark stems from the combined action of the alkali pre-treatment and the subsequent polyphenolic modification. The initial KOH stage cleans the fiber surface by stripping away lignin, hemicellulose, and waxy substances. This step successfully exposes more hydroxyl (–OH) groups and scours the surface to make it rougher. The follow-on application of tannic and gallic acids further strengthens the interface. These polyphenols act as a bridge, forming hydrogen bonds and potential ester linkages between the cellulose on the fiber and the carbonyl groups in the polymer matrix. This upgraded chemical interaction allows for more efficient stress transfer from the matrix to the fibers, leading to a composite that has fewer weak points at

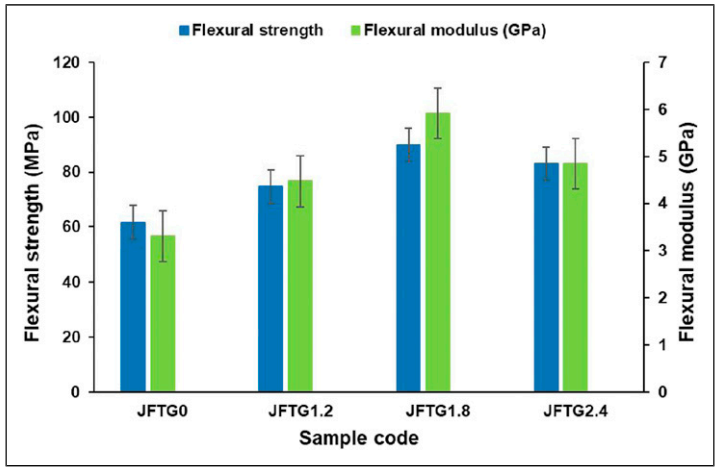

Figure 7. Influence of tannic and gallic acid concentration on the flexural properties of jute and flax biocomposites.

their junction. The optimal performance at 1.8% confirms that this concentration strikes the right balance between activating the fiber surface and preserving its inherent structure. When concentrations rise beyond this level, the fibers become overly coated with phenolic material and may even begin to degrade, leading to a loss of flexibility. In essence, optimising polyphenolic modification successfully strengthens the bond between the fibers and polymers. This approach directly produces tougher, more rigid bio-composites that maintain strong recyclability.

As Figure 8 illustrates, the success of this chemical bonding is visible in the uniform, tightly bound fracture surface. This specific morphology stems from the strong adhesion, which directly provides the composite with its enhanced structural integrity and ability to resist fracture.

Impact properties. Charpy impact testing was introduced to explain the fracture toughness of the hybrid biocomposites, quantifying the energy they absorb during a sudden fracture event. As shown in Figure 9, the application of tannic and gallic acid treatments consistently enhanced the material's impact property across all concentrations tested.

For the untreated JFTG0 specimen, the impact test measured an energy absorption of 7.71 kJ/m^2, presenting the performance baseline. Sample JFTG1.2, increased the energy absorption to 8.62 kJ/m^2, revealing an initial improvement in the strength between the fibers and the polymer. A further increase was recorded for the JFTG1.8 specimen, which registered 8.34 kJ/m^2. The most substantial performance gain was seen at the highest concentration, with the JFTG2.4 sample achieving an impact strength of 10.56 kJ/m^2. This peak in toughness implies that elevated acid levels foster superior interfacial adhesion, which in turn suppresses failure modes like fiber pull-out and debonding. This suppression of key failure modes allows the composite to

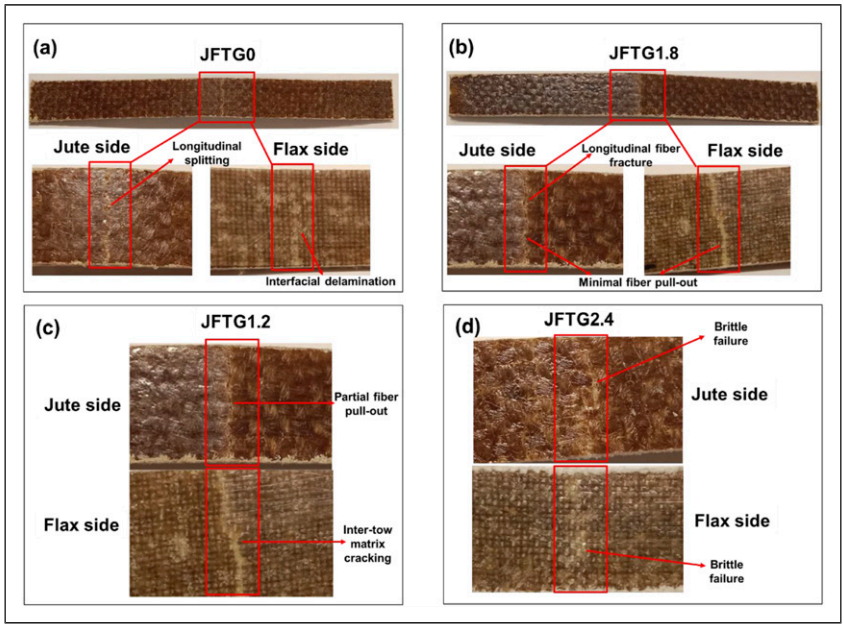

Figure 8. Top-surface flexural failure of various biocomposites (a) JFTG0, (b) JFTG1.8, (c) JFTG1.2, and (d) JFTG2.4.

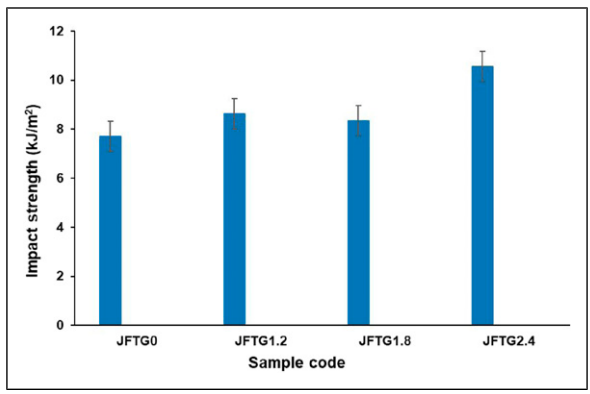

Figure 9. Impact strength of untreated and treated biocomposites.

endure greater energy absorption before cracking. This consistent rise in impact energy with increasing acid concentration directly supports the earlier tensile and flexural data. The treatments are responsible for this increased toughness, having created a more resilient interface through superior mechanical anchoring and chemical bonding. A

direct consequence of this strong bond is the efficient transfer of stress during high-speed impact.

The fracture surfaces in Figure 10 show the visual proof of this mechanism. Here, morphology shows a dual effect: the treatments successfully increase toughness, but at peak concentration, a trend toward brittleness emerges, changing the characteristic failure mode.

Surface and cross-sectional morphology of biocomposites via SEM. SEM analysis after Charpy pendulum impact test shows that the untreated laminate (JFTG0) exhibits a rough surface with micro-debris, fibre pull-outs, and weak interfacial consolidation, whereas tannic-acid and gallic-acid treatments (JFTG1.2, JFTG1.8, JFTG2.4) progressively produce a denser, more uniform surface with improved matrix coverage and reduced voids, especially at higher magnification (20 μm) as shown in Figure 11. Cross-sectional fracture observations as indicated in Figure 12 after Charpy impact further distinguish the samples: JFTG0 displays smooth fibre pull-out and interfacial debonding typical of brittle failure, while treated composites show rougher, more fibrillated fracture surfaces with stronger resin adhesion, fibre bridging, and reduced pull-out. The most pronounced interfacial integrity and energy-absorbing features such as matrix shear deformation and damaged fibre lumens appear in JFTG2.4, consistent with its improved impact strength. Overall, the morphological evolution with increasing acid concentration confirms that surface modification enhances fibre matrix bonding, minimises defects, and promotes tougher, more energy-dissipative fracture behaviour, directly supporting the observed improvement in impact resistance.

Abrasion properties. The 2-layer circular biocomposite laminates were fabricated from Elium resin and natural fibers, with a final diameter of 100 mm to meet the specifications of the Martindale abrasion tester. For the evaluation, a 26 mm head fitted with 400-grit sandpaper was used as the abrading surface. The mass loss (precision balance) and thickness change (vernier calipers) recorded at set intervals (Table 7) served as the basis for calculating the Abrasion Index (Ra) using equation (5). This metric provides a

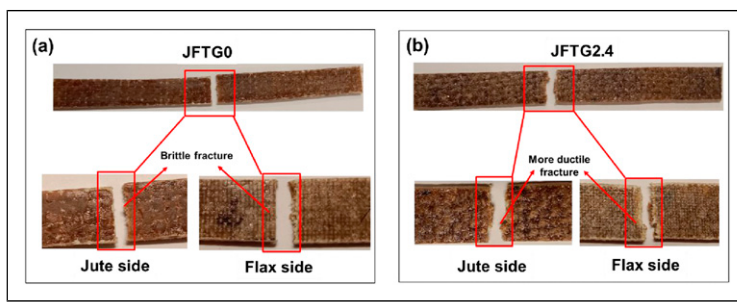

Figure 10. Impact characterised fractured samples (a) JFTG0, and (b) JFTG2.4.

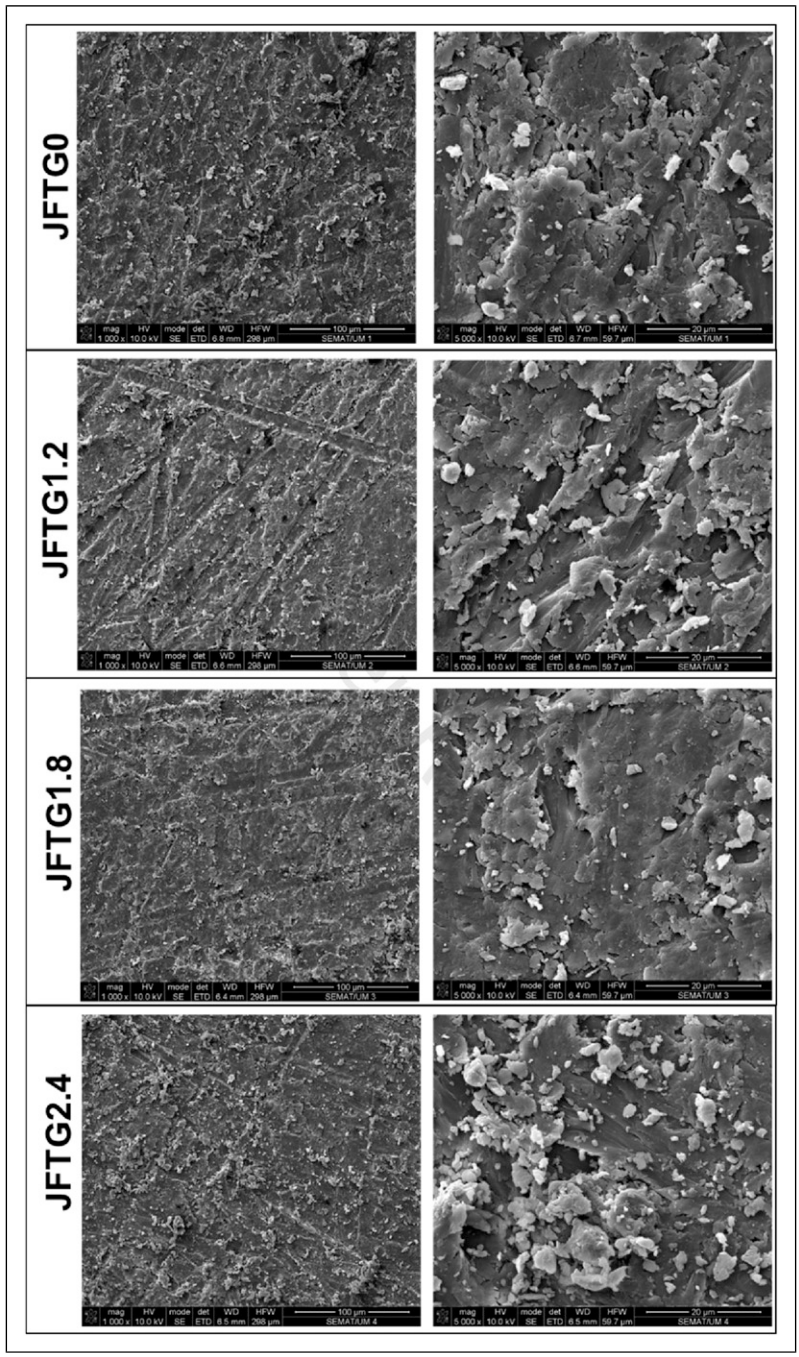

Figure 11. Surface analysis via SEM for various biocomposites.

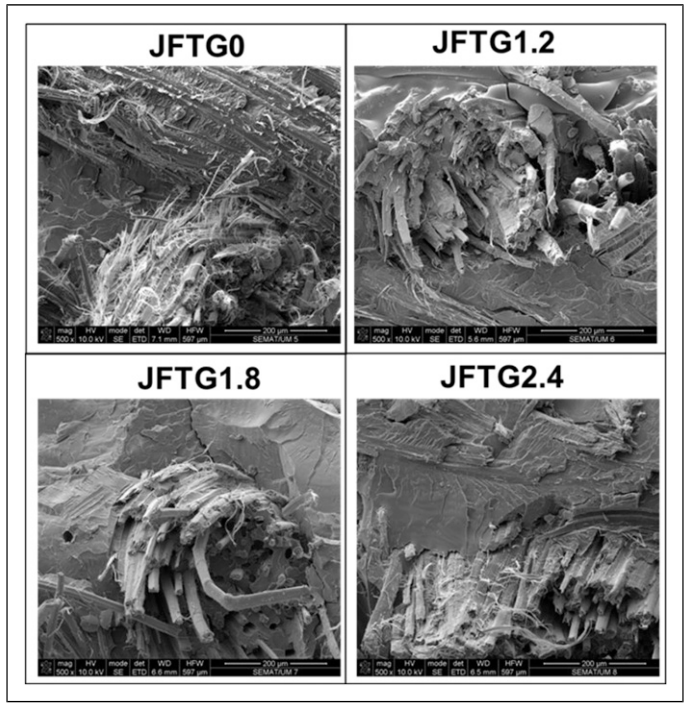

Figure 12. Cross-sectional analysis via SEM for various biocomposites.

quantitative measure of wear resistance by accounting for both volumetric losses derived from mass and thickness changes and surface degradation. Where constant k is 0.25.

$$Mass\ loss\ (\%) = \left(\frac{m_i - m_f}{m_i}\right) \times 100 \tag{2}$$

Since the abrader diameter = 26 mm, the contact area A_0 is:

$$A_0 = \left(\pi r^2\right) = \left(3.14 \times 13^2\right) = 530.93\, mm^2 \tag{3}$$

$$Area\ loss = 530.93 \times \frac{h_0 - h_f}{h_0} \tag{4}$$

$$R_a = k \times \frac{\left(\left(m_i - m_f\right)h_0\right)}{\left(m_i \times 530.93 \times \left(h_0 - h_f\right)\right)} \tag{5}$$

Across all samples, Ra increased as shown in Figure 13 with cycling, confirming progressive material removal during repeated abrasive contact. The data reveals a clear

Table 7. Mass and thickness changes during abrasion of 2-layer biocomposites.

Cycle (rev)	FF0 (Mass gm./ Thickness mm)	FF1.2 (Mass gm./Thickness mm)	FF1.8 (Mass gm./Thickness mm)	FF2.4 (Mass gm./Thickness mm)	JJ0 (Mass gm./ Thickness mm)	JJ1.2 (Mass gm./ Thickness mm)	JJ1.8 (Mass gm./ Thickness mm)	JJ2.4 (Mass gm./ Thickness mm)
0	9.15/0.83	8.04/0.79	8.52/0.83	8.37/0.80	10.39/1.00	9.73/1.05	9.2/1.20	9.76/1.15
250	9.05/0.78	8.00/0.78	8.50/0.82	8.31/0.795	10.24/0.96	9.69/1.03	9.19/1.18	9.71/1.14
500	9.00/0.75	7.98/0.77	8.48/0.80	8.27/0.790	10.20/0.94	9.65/1.02	9.13/1.17	9.65/1.13
1000	8.95/0.74	7.93/0.76	8.44/0.79	8.24/0.780	10.12/0.93	9.57/1.01	9.04/1.15	9.61/1.11
1500	8.88/0.73	7.90/0.73	8.37/0.77	8.18/0.770	10.06/0.90	9.50/0.99	8.96/1.12	9.57/1.10
2000	8.82/0.72	7.84/0.70	8.32/0.75	8.16/0.760	10.01/0.88	9.46/0.96	8.89/1.09	9.50/1.08
2500	8.75/0.71	7.82/0.68	8.25/0.74	8.14/0.750	9.89/0.86	9.39/0.94	8.80/1.08	9.48/1.06

performance gap: flax-Elium (FF) biocomposites generally offered better abrasion resistance than jute-Elium (JJ) ones, as evidenced by their lower Ra values. For the jute series, increasing the treatment level (e.g., JJ1.8, JJ2.4) correlated with higher Ra, indicating diminished abrasion stability. The FF2.4 specimen was a clear outlier, beginning with a high Ra value that steadily dropped. This pattern is consistent with the early-stage removal of a fragile surface layer, followed by the exposure of a more wear-resistant core. The FF0 and FF1.2 samples, however, showed the greatest consistency, with their Ra values changing very little between the initial and final measurements.

Thermal behavior of biocomposites. The TGA curves as shown in Figure 14 of the Elium-based hybrid biocomposites exhibit a small mass loss below ~120°C attributed to removal of absorbed moisture and low-molecular volatiles, followed by a single major degradation step between ~300 and 430°C. The onset of significant degradation (≈5 % mass loss) occurs around 290-300°C for all laminates and is slightly shifted to higher temperature for the acid-treated samples (JFTG1.2 to JFTG2.4), indicating a marginal improvement in thermal stability compared with the untreated composite (JFTG0). DTG traces show a shoulder at ~250-280°C due to hemicellulose degradation and a main peak at ~360-380°C corresponding to the simultaneous decomposition of Elium matrix and the cellulose/lignin fractions. The treated composites, particularly JFTG1.2 and JFTG1.8, present slightly higher Tmax and peak intensities together with a modest increase in char residue (~8 to 10 wt% at 600°C), which can be related to enhanced fiber-matrix interactions and the additional aromatic char from tannic/gallic acids, without changing the overall degradation mechanism.

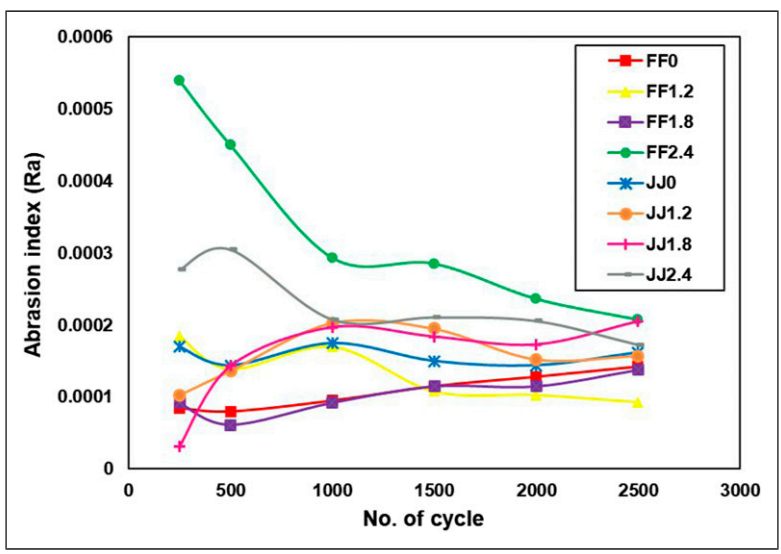

Figure 13. Progression of surface roughness (Ra) as a function of abrasion cycles for 2-layer thermoplastic biocomposites.

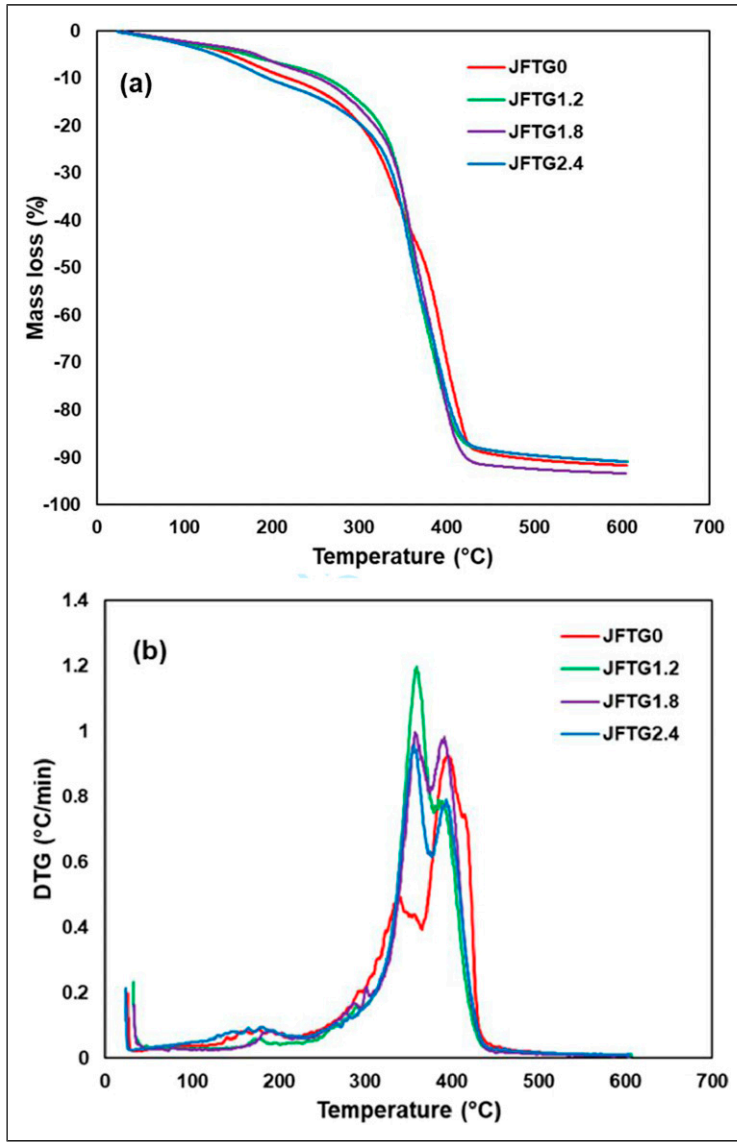

Figure 14. TG (a) and DTG (b) curves for untreated and treated biocomposites with different concentrations of acids.

Numerical simulation and model validation

In this work, numerical modeling of the fundamental mechanical properties of natural fiber-reinforced thermoplastic composites, both untreated and chemically treated with tannic and gallic acids, was performed, and the results were validated against

experimental data. Numerical 3D modeling was performed in Ansys LS-DYNA Suite R16.1 Student program, which is limited to a maximum total number of 128×10^3 nodes/elements. Tensile and three-point bending tests were conducted, the schematic of which are illustrated in Figure 15.

The specimens and the indenter were modeled with shell elements (fully integrated shell element ELFORM = 16) using the finite element method. One end of the tensile specimen was fixed as immovable. A coarser mesh of 2.5 × 1.25 mm was selected in the grip regions, while a uniform mesh of 1.25 × 1.25 mm was applied elsewhere. The tensile specimen consisted of a total of 2800 elements (2961 nodes). Seven integration points through the specimen thickness were selected (NIP = 7). In contrast, the bending specimen was modeled with a uniform finite element mesh of 1.3 × 1.25 mm. The bending specimen consisted of 960 elements (1067 nodes), with nine integration points selected (NIP = 9). The indenter consisted of 480 elements (512 nodes), and the two supports together consisted of 960 elements (1024 nodes). All directions of movement of the indenter were restricted except for vertical movement, and the supports were fully constrained in all degrees of freedom. In contrast, the composite required no additional restraint as it was compressed from above by the indenter while resting on both supports from below. Frictional forces acted between the metal surfaces and the test specimen.

AUTOMATIC_SURFACE_TO_SURFACE contact was selected for the bending test. The following friction coefficients were adopted: static and dynamic friction coefficients μs = 0.5 and μd = 0.35, respectively, and exponential decay coefficient DC = 7.52.

During tensile testing, equivalent von Mises stresses were evaluated, while for more complex bending deformation, strain energy density (SED) was additionally assessed. SED equals the area under the stress-strain curve and represents the strain energy stored in a material per unit volume (SI unit: J m^{-3})[14,15]:

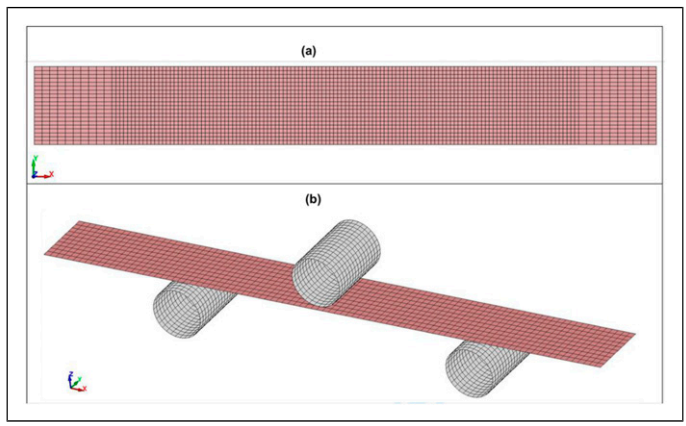

Figure 15. Finite element mesh of the tensile specimen (a) and three-point bending test configuration (b).

$$SED = \int_0^{\varepsilon_{peak\_F}} \sigma(\varepsilon) d\varepsilon \tag{6}$$

where ε_{peak_F} denotes the strain at maximum force.

The experimental and numerical tensile test curves are presented in Figure 16. As can be seen, all composite tensile stress-strain curves coincide with numerical curves with sufficient accuracy. The shape of the deformation curves is similar. Following a short linear region, the curves bend and increase steadily until maximum load is reached. The tensile stress-strain curves are relatively smooth. Uniaxial tension subjects the entire gauge section to uniform tensile stress, which tends to produce more synchronized damage accumulation and consequently smaller amplitude oscillations. The fiber pull-out mechanism dominates. The weaker fiber-matrix interface allows fibers to be extracted from the matrix rather than transferring stress efficiently until fiber fracture. As the load increases, multiple fibers gradually disengage rather than experiencing the abrupt interfacial shear failures characteristic of bending-induced stress concentrations. Matrix microcracking contributes to the serrated behavior by creating sudden compliance changes and localized stress redistributions.

Tensile curves of all specimens show largely brittle behavior (clear, sharp peak and abrupt drop in load at fracture). Sample JFTG2.4 (Figure 16(d)) shows the largest strain-to-failure (a bit more ductile) but still fails in a brittle-looking way (fiber fracture rather than progressive pull-out). Tensile curves of sample JFTG0 (untreated) and sample JFTG2.4 (highest TA/GA) are similar, sample JFTG2.4 has slightly higher strain-to-

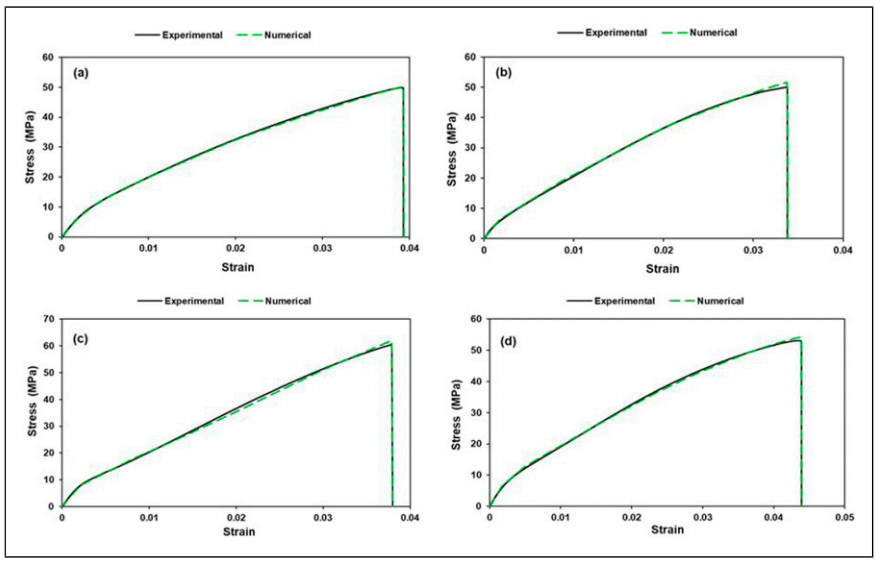

Figure 16. The experimental and numerical tensile test curves (a) JFTG0, (b) JFTG1.2, (c) JFTG1.8, (d) JFTG2.4.

failure. However, flexural curves of JFTG0 and JFTG2.4 differ a lot across samples. Meanwhile, samples JFTG1.2 and JFTG1.8 (intermediate TA/GA) doses) are like each other in both tension and flexure, but they differ from JFTG0 and JFTG2.4. Such pattern shows a bimodal response: JFTG0 and JFTG2.4 behave similarly in tension, while JFTG1.2 and JFTG1.8 form a second group; flexural responses are more sensitive and spread out. A mechanistic explanation reveals two different competing effects that TA/GA acid can produce in a laminate: (1) interfacial strengthening and (2) fiber-matrix modification or residual effects. Molecules adsorb onto fiber surfaces and improve bonding to resin. This increases initial stiffness transfer and peak strengths. However, depending on dose and processing, the treatment can (a) plasticize the adjacent matrix (more ductile interphase), (b) locally stiffen (crosslink) the interphase (more brittle), or (c) leave acid residues that affect cure or fiber integrity (damage/weakness). Because these effects depend nonlinearly on concentration and deposition uniformity, a small increase in dose may push the system from one regime to another explaining why mid doses (samples JFTG1.2 and JFTG1.8) behave similarly to each other, but differently from untreated (JFTG0) or high (JFTG2.4) dose. Two different physical routes can produce similar tensile curves of sample JFTG0 (untreated) and sample JFTG2.4 (highest dose) in tension. Being chemically untreated, sample JFTG0 has lower interfacial shear strength (IFSS), its peak in tension is lower and failure is dominated by fiber pull-out (progressive failure).

When evaluating the maximum tensile stress (Table 8), regardless of the composite, the numerical result differed from the simulation by 0.55-3.18%. Meanwhile, when evaluating the maximum flexural deformation, the result differed by 0.53-1.71%.

Flexural capacity is relatively lower but more gradual plasticity is observed. Sample JFTG2.4 looks untreated in tensile, tensile curve is similar to sample JFTG0 in shape but with slightly larger strain-to-break, which suggests matrix plasticization or non-uniformity. This could be explained by two opposite effects: improved fiber bonding vs. embrittlement/acid residue or plasticization. With higher TA/GA dose there is over-coating or aggregation, meaning that excessive acids form thick, brittle surface layers or aggregates that reduce effective interfacial bonding (heterogeneous and weak adhesion), so load transfer is not uniformly enhanced effective macro response close to untreated. Secondly, matrix plasticization could be dominating, meaning high dose diffuses

Table 8. Comparison of maximum stress σmax results obtained by experiment and numerical modeling.

	Tensile			Flexural		
Sample	Experiment	Numerical	Diff. %	Experiment	Numerical	Diff. %
JFTG0	49.91	50.18	0.55	62.41	61.35	1.71
JFTG1.2	50.05	51.64	3.18	74.60	73.66	1.25
JFTG1.8	60.57	61.97	2.32	86.40	85.18	1.42
JFTG2.4	53.14	54.23	2.05	83.22	82.78	0.53

(residues plasticize) the nearby matrix, lowering elastic stiffness locally and increasing strain to failure. The peak stress ends up not much higher than untreated, but the failure mode shifts, producing similar tensile curves with slightly higher strain-to-failure. In contrast, under loading conditions other than pure tension, different behavior is observed. The experimental and numerical test curves for bending are presented in Figure 17.

As observed, the flexural curves differ markedly (JFTG0 and JFTG2.4) even when the tensile curves are similar (JFTG0 and JFTG2.4). The flexural response is matrix- and interphase-dominated, governed by fiber buckling, kinking, and localized matrix flow. Even minor variations in interphase toughness or matrix plasticity produce substantial differences in flexural strain capacity and the shape of the flexural stress-strain curve. If treatment induces matrix plasticization or causes incomplete cure due to residues as is plausible in sample JFTG2.4 the flexural behavior may exhibit greater ductility (higher strains) because the matrix yields and accommodates large deformations without catastrophic fiber kinking.

Samples JFTG1.2 and JFTG1.8 have improved peak strength and appear similar in deformation behavior, both in tension and flexure. At 1.2% and 1.8% TA/GA the chemistry and surface coverage may be in a similar regime: sufficient adsorption (more uniform deposition) significantly increases IFSS, but not so much that the interphase becomes embrittled or resin cure is affected. This results in samples JFTG1.2 and JFTG1.8 showing similar deformation responses relative to untreated (higher peak, altered post-peak). The interface hardening (fracture toughness) seems to be comparable hence similar curves. If treatment stiffens interface, flexural load is carried more

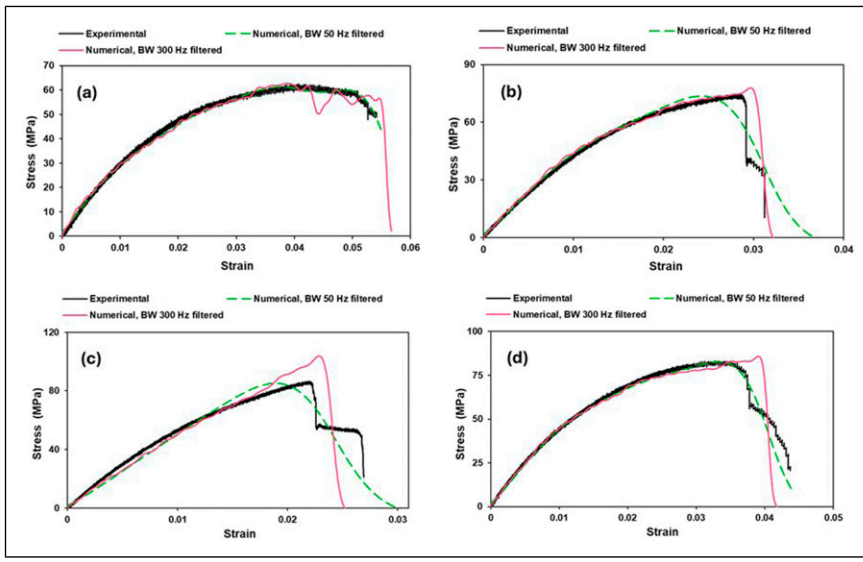

Figure 17. The experimental and numerical bending test curves (a) JFTG0, (b) JFTG1.2, (c) JFTG1.8, (d) JFTG2.4.

effectively but failure can be more brittle (lower flexural strain to failure) or show different hardening.

From the numerical tensile results, it can be observed that localized stress concentration occurs at the specimen grip ends (small red zones), with stresses distributed symmetrically at both ends. In the numerical model, the ends are ideally constrained, whereas the actual constraint differs to some extent. Moreover, the actual specimen exhibits fiber waviness, resin inhomogeneities, surface defects, microcracks, non-uniform matrix-fiber adhesion, regions of varying specimen thickness, and similar imperfections. In the numerical model, the specimen fails at either the fixed or moving end, whereas the actual specimen may fail at the center if a weaker region develops there, even though stress at the ends may be somewhat higher. Based on the deformation-strain tensile curves and their agreement with the numerical results, when appropriate composite properties are assigned, the mechanical behavior of such composites can be estimated with sufficient accuracy. From Figure 18(c), it is evident that prior to failure, the von Mises stresses in composite JFTG1.8 are the highest (peak ~84.5 MPa), with the most uniform stress distribution. This indicates that the composite is stiff and likely exhibits brittle (matrix-dominated) behavior. In contrast, composites shown in Figure 18(a), (b), and (d) exhibit lower and relatively similar stresses (60-64 MPa). The maximum von Mises stresses σVM for composites JFTG1.2 and JFTG2.4 are comparable (approximately 64 MPa), suggesting that treatment with a higher acid concentration of 2.4% was not as effective as treatment with 1.8% concentration regarding tensile strength. Treatment with 1.2% acid concentration contributed only marginally to increased composite tensile strength. It should be noted that this composite JFTG1.2 began to fail earliest (element deletion started at 33.75 ms). The low acid concentration may have resulted in a suboptimal layer and non-uniform coverage, which could explain the earliest failure time.

The von Mises stresses for bending specimens are illustrated in Figure 19. High strain energy density (SED) values, distribution over a larger area, and moderate von Mises stresses indicate good energy dissipation. As can be observed from Figure 19(a), the σVM stresses are distributed over a relatively large area accompanying a high SED value (236 kJ m^{-3}). Thus, when deforming the chemically untreated composite JFTG0, energy dissipates across a wide zone via matrix microcracking, fiber debonding, and pull-out. This indicates good composite toughness and stable damage progression (ductile flexural response). In contrast, when bending the composite JFTG1.2 with 1.2% treatment (Figure 19(b)), the σVM stresses are relatively high (32.33 MPa) and concentrated. Additionally, although the SED is moderate (160 kJ m^{-3}), it is distributed in a very small zone. This suggests that treatment at 1.2% is probably inconsistent or produces defects (inhomogeneous interface), which lead to localized stress concentration and earlier failure. The tensile strength (Figure 16(b)) is somewhat higher than that of the JFTG0 composite (Figure 16(a)), indicating reduced ductility. Meanwhile, when bending the composite treated with 1.8% (Figure 19(c)), the lowest SED value is obtained (72.6 kJ m^{-3}), although the σVM stresses are distributed over a large zone, like the untreated composite. This composite has the highest tensile σmax (60.6 MPa) and very high von Mises stresses in tension (84.4 MPa, Figure 18(c)). This indicates that chemical treatment at this level maximized interfacial bonding and axial load transfer, causing fibers to break

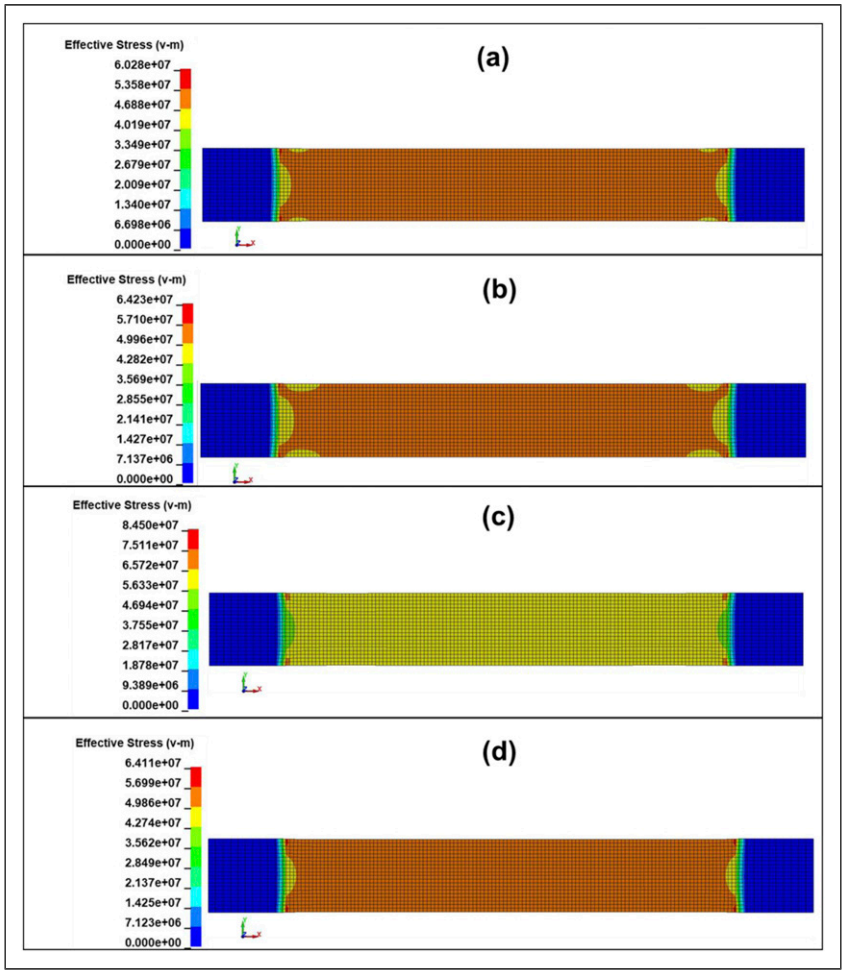

Figure 18. Equivalent von Mises stresses in SI units Pa at 0.01 ms before the start of failure (start of element deletion) after dynamic tensile test simulation: (a) JFTG0 (39.26 ms), (b) JFTG1.2 (33.74 ms), (c) JFTG1.8 (37.88 ms), (d) JFTG2.4 (43.84 ms).

at higher loads (excellent tensile strength). However, the bending test results show very low bending SED and brittle bending failure. This indicates that the treatment also had a negative effect, as fiber pull-out/slip and energy dissipation were reduced. This could have been influenced by the removal of amorphous, ductile constituents (hemicellulose), the formation of a stiff and brittle interfacial layer (adsorbed phenolics), or the introduction of micro-notches. In contrast, the composite with 2.4% treatment showed high tensile ductility (largest strain to failure ε, Figure 19(d)), moderate-to-high SED (203.8 kJ m^{-3}), and relatively high σVM, though distributed over a smaller area. All of this indicates that

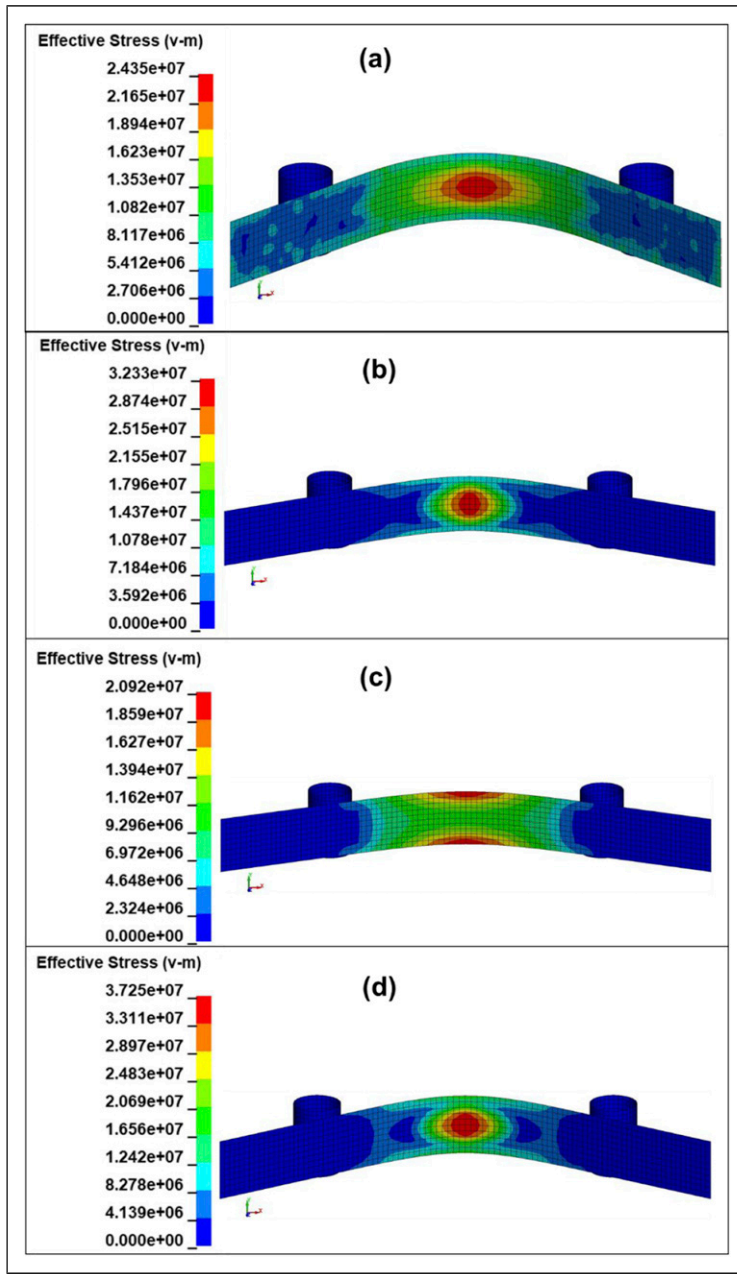

Figure 19. Equivalent von Mises σVM stresses in SI units Pa at 0.01 ms before the onset of failure (start of element deletion) after performing a dynamic 3-point bending test simulation: (a) JFTG0 (56.53 ms), (b) JFTG1.2 (31.06 ms), (c) JFTG1.8 (24.11 ms), (d) JFTG2.4 (40.54 ms). The top view is rotated 20° from the viewer.

the highest concentration promotes good interfacial bonding, providing good strength and good energy absorption.

Conclusion

This investigation establishes that treating natural fibers with biodegradable acids substantially improves the mechanical performance of thermoplastic biocomposites. Both experimental tests and computer simulations identified 1.8% as the ideal concentration for tannic and gallic acids, achieving maximum enhancement in tensile strength, flexural modulus, and impact resistance while preserving fiber structure. Performance diminished at 2.4% concentration, revealing that excessive treatment damages composite properties. These outcomes verify that biodegradable acid treatments represent a viable eco-friendly method for upgrading biocomposite performance suitable for sustainable applications such as lightweight automotive interior panels, biodegradable consumer packaging, and eco-friendly structural panels in building and construction. Subsequent work will prioritize scaling production and verifying the material's long-term performance under actual operating conditions.

Author contributions

Sultan Ullah: Conceptualization, Methodology, Data collection for Simulation & Validation, Writing – original draft preparation, Simulation Analysis, Fabrication, & Testing. **Giedrius Janusas:** Conceptualization, Supervision. **Christopher M Pastore:** Review & Visualization. **Raul Fangueiro:** Conceptualization, Resources. **Arvydas Palevicius:** Conceptualization, Resources. **Almontas Vilutis:** Simulation, Verification & Analysis. **Sandra Varnaitė-Žuravliova**: Testing, Resources. **Justas Eimontas:** Testing, Collection.

Declaration of conflicting interests

The authors declared no potential conflicts of interest with respect to the research, authorship, and/or publication of this article.

Funding

The authors received no financial support for the research, authorship, and/or publication of this article.

ORCID iD

Sultan Ullah https://orcid.org/0000-0003-1233-1926

Data Availability Statement

The authors confirm that the data supporting the findings of this study are available within the article.

References

1. Sun Z, Duan Y, An H, et al. Research progress and application of natural fiber composites. *J Nat Fibers* 2023; 20: 2206591.
2. Ullah S, Akhter Z, Palevičius A, et al. Review: natural fiber based biocomposites for potential advanced automotive applications. *J Eng Fibers Fabrics* 2025; 20: 1–25.
3. Feng Y, Hao H, Lu H, et al. Exploring the development and applications of sustainable natural fiber composites: a review from a nanoscale perspective. *Composites Part B* 2024; 276: 111369.
4. Ali A, Shaker K, Nawab Y, et al. Hydrophobic treatment of natural fibers and their composites: a review. *J Ind Text* 2018; 47: 2153–2183.
5. Nagaraja S, Anand PB, Mohan Kumar K, et al. Synergistic advances in natural fibre composites: a comprehensive review of the eco-friendly bio-composite development, its characterization and diverse applications. *RSC Adv* 2024; 14: 17594–17611.
6. Kamarudin SH, Basri MSM, Rayung M, et al. A review on natural fiber reinforced polymer composites (NFRPC) for sustainable industrial applications. *Polymers* 2022; 14: 3698.
7. Sai KKV, Achyuth P, Reddy MVJ, et al. Enhancement of mechanical prop-erties of coir, kapok, and hemp fiber-reinforced epoxy composites for a variety of Ap-plications. *Mechanics of Advanced Composite Structures* 2026; 13(2): 271–281.
8. Muthalagu R, Sathees Kumar S, Pati PR, et al. Influence of Prosopis juliflora bark powder/fillers on the mechanical, thermal and damping properties of jute fabric hybrid composites. *J Mater Res Technol* 2024; 33: 3452–3461.
9. Purohit A, Dehury J, Sitani A, et al. A novel study on the stacking sequence and mechanical properties of jute-kevlar-epoxy composites. *Interactions* 2024; 245: 100.
10. Torres FG, Arroyo OH and Gomez C. Processing and mechanical properties of natural fiber reinforced thermoplastic starch biocomposites. *J Thermoplast Compos Mater* 2007; 20(2): 207–223.
11. Mukhopadhyay SC and Fangueiro R. Physical modification of natural fibers and thermoplastic films for composites — a review. *J Thermoplast Compos Mater* 2009; 22(2): 135–162.
12. Skosana SJ, Khoathane C and Malwela T. Driving towards sustainability: a review of natural fiber reinforced polymer composites for eco-friendly automotive light-weighting. *J Thermoplast Compos Mater* 2024; 38(2): 754–780.
13. Gholampour A and Ozbakkaloglu T. A review of natural fiber composites: properties, modification and processing techniques, characterization, applications. *J Mater Sci* 2020; 55: 829–892.
14. Verma D and Goh KL. Effect of mercerization/alkali surface treatment of natural fibres and their utilization in polymer composites: mechanical and morphological studies. *J Compos Sci* 2021; 5: 175.
15. Chandramohan D, Murali B, Vasantha Srinivasan P, et al. Mechanical, moisture absorption, and abrasion resistance properties of bamboo–jute–glass fiber composites. *J Bio Tribocorros* 2019; 5: 66.
16. Li X, Tabil LG and Panigrahi S. Chemical treatments of natural fiber for use in natural fiber-reinforced composites: a review. *J Polym Environ* 2007; 15: 25–33.

17. Amin MN, Ahmad W, Khan K, et al. A comprehensive review of types, properties, treatment methods and application of plant fibers in construction and building materials. *Materials* 2022; 15: 4362.
18. Gupta MK, Ramesh M and Thomas S. Effect of hybridization on properties of natural and synthetic fiber-reinforced polymer composites (2001–2020): a review. *Polym Compos* 2021; 42: 4981–5010.
19. Heckadka SS, Nayak SY, Joe T, et al. Comparative evaluation of chemical treatment on the physical and mechanical properties of areca frond, banana, and flax fibers. *J Nat Fibers* 2022; 19: 1531–1543.
20. Das PP, Manral A, Ahmad F, et al. Environmentally sustainable chemical treatment of plant fibers for improved performance of polymeric composites. *Polym Compos* 2022; 43: 6711–7632.
21. Jawalkar CS and Kant S. Critical review on chemical treatment of natural fibers to enhance mechanical properties of bio composites. *Silicon* 2021; 14: 5103–5124.
22. Wu Y, Xia C, Cai L, et al. Development of natural fiber-reinforced composite with comparable mechanical properties and reduced energy consumption and environmental impacts for replacing automotive glass-fiber sheet molding compound. *J Clean Prod* 2018; 184: 92–100.
23. Pinto Â, Esteves D, Nobre L, et al. Mechanical performance enhancement in natural fibre reinforced thermoplastic composites through surface treatment and matrix functionalisation. *Polymers* 2025; 17: 532.
24. Sahu P and Gupta M. A review on the properties of natural fibres and its bio-composites: effect of alkali treatment. *Proc Inst Mech Eng Part L J Mater Des Appl* 2019; 234: 198–217.
25. Ullah S, Palevičius A, Janusas G, et al. Enhancing mechanical and impact properties of flax/glass and jute/glass hybrid composites through KOH alkaline treatment. *Polymers* 2025; 17: 804.
26. Chandrasekar M, Ishak MR, Sapuan SM, et al. A review on the characterisation of natural fibres and their composites after alkali treatment and water absorption. *Plast Rubber Compos* 2017; 46: 119–136.
27. Zhao XL, Hou GX, Yu SW, et al. Preparation of HNTs d GO hybrid nanoparticles for gallic acid epoxy composites with improved thermal and mechanical properties. *Polym Compos* 2022; 43: 5133–5145.
28. Butt MS, Shaker K, Asghar MA, et al. Shaping sustainable pathways: enhancing mechanical properties of biocomposite through tannic acid treatment of flax fabrics. *Int J Biol Macromol* 2024; 266(Pt 2): 131393.
29. Pantaleoni A, Marrocchi A, Russo P, et al. Advanced flame retardant biocomposites: polylactic acid reinforced with green gallic acid iron phosphorus coated flax fibers. *Int J Biol Macromol* 2025; 300: 140215.
30. Venkatesan R, Dhilipkumar T, Shankar KV, et al. Eco friendly food packaging: gallic acid as a cross linking agent in PBAT/Cellulose composite films. *Cellulose* 2024; 31: 8105–8125.
31. Haroun AA and El Toumy SA. Effect of natural polyphenols on physicochemical properties of cross linked gelatin based polymeric biocomposite. *J Appl Polym Sci* 2010; 116: 2825–2832.
32. Zhang M, Jin L, Zhai Y, et al. Bio inspired gallic acid gelatin coating: a novel strategy for ecofriendly interfacial modification of carbon fibre composites. *Compos Commun* 2021; 26: 100790.

33. Croitoru AM, Ayran M, Altan E, et al. Development of gallic acid loaded ethylcellulose fibers as a potential wound dressing material. *Int J Biol Macromol* 2023; 253: 126996.
34. Liu L, Xu X, Wu J, et al. Preparation of gallic acid–polydimethylsiloxane codeposited carbon fibers to improve interfacial properties of epoxy composites. *J Reinforc Plast Compos* 2024; 44: 35–49.
35. Pishva B, Nourmohammadi J and Hesaraki S. Gallic acid grafted hybrid strontium fluoride/polycaprolactone nanocomposite fibers for bone regeneration. *Prog Org Coating* 2022; 170: 106976.
36. Chen S, Lv S, Hou G, et al. Mechanical and thermal properties of biphenyldiol formaldehyde resin/gallic acid epoxy composites enhanced by graphene oxide. *J Appl Polym Sci* 2015; 132: 42637.
37. Yin Y, Huang Z, Wang P, et al. The use of copper ions and tannic acid to enhance the UV protection of cotton fabrics. *J Nat Fibers* 2022; 19: 3492–3501.
38. Kamaludin NHI, Ismail H, Rusli A, et al. Properties enhancement of chitosan filled polylactic acid biocomposites using tannic acid treatment. *Polym Compos* 2022; 43: 21–35.
39. Shibata M and Nakai K. Preparation and properties of biocomposites composed of bio-based epoxy resin, tannic acid, and microfibrillated cellulose. *J Polym Sci, Part B: Polym Phys* 2010; 48: 425–433.
40. Kim YO, Cho J, Kim YN, et al. Recyclable, flame retardant and smoke suppressing tannic acid-based carbon fiber reinforced plastic. *Composites Part B* 2020; 197: 108173.
41. Hu W, Yang L, Wang F, et al. Insight into the enhanced interfacial adhesion of carbon fiber reinforced composites: a facile ferric ion and tannic acid self-assembly strategy. *Composer Part A Appl Sci Manuf* 2024; 177: 107926.
42. Xiang D, Chen C, Xie G, et al. Tannic acid and aminopropyltriethoxysilane modified basalt fiber/epoxy resin composites with enhanced interfacial and mechanical properties. *Polym Compos* 2025; 46: 1108–1122.
43. Singh AS, Halder S, Wang J, et al. Tannic acid intermediated surface functionalization of bamboo micron fibers to enhance mechanical performance of hybrid GFRP. *Composites Part B* 2019; 177: 107322.
44. Liu W, Qiu J, Chen T, et al. Regulating tannic acid crosslinked epoxidized soybean oil oligomers for strengthening and toughening bamboo fibers reinforced poly (lactic acid) biocomposites. *Compos Sci Technol* 2019; 181: 107709.
45. Asim M, Paridah MT, Chandrasekar M, et al. Thermal stability of natural fibers and their polymer composites. *Iran Polym J (Engl Ed)* 2020; 29: 625–648.
46. Wang X, Yang G and Guo H. Tannic acid as biobased flame retardants: a review. *J Anal Appl Pyrolysis* 2023; 174: 106111.